Catalysis Science & Technology

Accepted Manuscript

ROYAL SOCIETY OF CHEMISTRY

www.rsc.org/catalysis

Catalysis Science & Technology RSCPublishing

ARTICLE

Highly efficient and chemoselective hydrogenation of α, β-unsaturated carbonyls over Pd/N-doped hierarchically porous carbon

Cite this: DOI: 10.1039/x0xx00000x

Received 00th January 2014,
Accepted 00th January 2014

DOI: 10.1039/x0xx00000x

www.rsc.org/

Zhongzhe Wei, Yutong Gong, Tianyi Xiong, Pengfei Zhang, Haoran Li, Yong Wang*

Palladium nanoparticles supported on a N-doped hierarchically porous carbon, Pd/CNx, has been developed as a highly efficient, reusable and environmentally benign heterogeneous catalyst for the selective hydrogenation of various α, β-unsaturated carbonyls to their corresponding saturate carbonyls at mild conditions (303 K, atmospheric H_2). Complete conversion of a series of α, β-unsaturated carbonyls with excellent selectivity (>99%) was achieved within 4 h. Moreover, the catalyst can be easily recovered by centrifugation and withstands recycling up to 8 times without apparent loss of activity and selectivity. The considerable catalytic performance is attributed to the hierarchically porous network and incorporation of nitrogen atoms. This catalytic system opens up an efficient, selective, recyclable and sustainable method for selective hydrogenation process.

Introduction

Chemoselective hydrogenation of α, β-unsaturated carbonyls is fundamentally important as its extensive applications in the synthesis of fine chemicals, pharmaceuticals and functional materials.[1-4] The selectivity varies due to the possibility of hydrogenation of either the C=C bond or the C=O band, or both of them (Scheme 1). The selective hydrogenation of C=C bond is an important industrial process in which heterogeneous catalysts especially supported precious metal catalysts have been attached much attention for the ease of their separation and recycling together with their outstanding performance.[5-7] Supported palladium catalysts are widely used for the reaction. For example, Lakshmi *et al* reported that layered double hydroxides supported Pd was used as a heterogeneous catalyst for olefinic bond hydrogenation with high selectivity.[8] Content catalytic performance over polysiloxane-encapsulated Pd nanoclusters for the hydrogenation of functional conjugated alkenes was observed by Bandoo *et al*.[9] Bhanage *et al* also applied polymer-supported catalytic system, polymer-supported Pd-*N*-heterocyclic carbine, for the chemoselective conjugate reduction of α, β-unsaturated carbonyls at 100 °C.[10] The advantages of both homogeneous and heterogeneous catalysts were achieved when supported catalysts with the aid of ionic liquids were carried out in the selective reduction of C=C bond.[11-14] To get better performance of catalysts, additives sometimes are inevitable. Pd/C together with various additives like pyridines, amines and diphenylsulfide that resulted in the selective hydrogenation of C=C bond was subsequently reported.[15] Bimetallic catalysts have also received intense interest because of possible synergistic effect which makes selective hydrogenation reactions easier. Xu and co-workers disclosed that a small amount of fully dispersed Pt entities loaded on Au nanoparticles provided dramatic activity enhancement for the chemoselective hydrogenation of α, β-unsaturated carbonyls.[16] The similar effect was also illustrated in the Ni/TiO_2 doping with a tiny amount of Ir for the hydrogenation of cinnamaldehyde (CAL) to hydrocinnamaldehyde (HCAL) under 2 MPa H_2 at 80 °C.[17] Li *et al* applied water-soluble Pt_xNi_{1-x} ($0<x<1$) to the hydrogenation of C=C bond in benzalacetone, and got excellent yield.[18] Despite all of these well-established methodologies, the development of a highly effective, selective and environmentally benign heterogeneous catalyst under mild conditions is highly desirable.

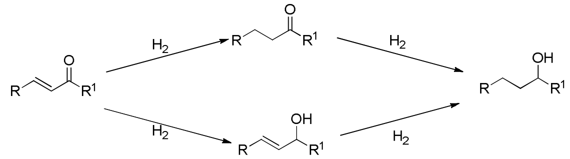

Scheme 1. Reaction pathways for the hydrogenation of α, β-unsaturated carbonyls.

In the construction of heterogeneous catalysts to selectively reduce C=C bond in α, β-unsaturated carbonyls, Pd is conventionally used as the catalytic center, which is confirmed by experimental results[8, 19, 20] and theoretical work.[21-23] It is well recognized that the nature of supports has a significant effect on the activity and selectivity behavior of the catalysts.[24, 25] The catalytic activity of a heterogeneous catalyst can be enhanced by suitably controlling and selecting the support.[26] Hence, the choice of support is vital. Carbon materials, including activated carbon, carbon nanofibers and hydrophilic carbon, etc., are good supports for heterogeneous catalysts because of specific properties. [27-30] Commercial Pd/C can catalyze the selective hydrogenation of CAL, but the apparent rate of the reaction is low and the selectivity toward HCAL remains poor.[27, 31] This could be explained that activated microporous carbon materials may depress the mass transport of molecules because of space confinement imposed by small pore sizes.[32] To overcome the limitations, efforts have been directed towards mesoporous carbon materials, especially hierarchically structured porous materials.[33] Thanks to much less diffusion restriction in mesoporous structures for molecules and greatly shortened diffusion distances in the channels, the catalysts with hierarchically porous structure exhibit high catalytic behavior.[34] However, noble metals deposited on carbons easily leach during catalytic processes because the interaction between the metal nanoparticles and the carbon surface is always weak, hence modification of carbons is necessary.[35] In this respect, doping with heteroatoms in carbon is regarded as an impressive strategy. Nitrogen-doped carbon materials have attracted worldwide attention recently due to an even wider range of applications than carbon materials, such as oxygen reduction reaction,[36] catalyst support,[37] etc. The incorporation of nitrogen atoms may not only enhance the electronic density of supported metal nanoparticles, but also provide more structural defects.

Very recently, we successfully designed fascinating N-doped carbon (CN) materials with hierarchical structure from glucose by hydrothermal carbonization procedure, which was a green and sustainable process.[37, 38] In search for a suitable catalyst for the chemoselective hydrogenation of α, β-unsaturated carbonyls, we anticipated that Pd/CN could exhibit interesting catalytic activity due to the hierarchically porous structure of the CN and the special catalyst support – metal heterojunction. Herein, we employed Pd/CN as an efficient catalyst for the selective hydrogenation of C=C bond using benign H_2 as the reduction agent. The activity of the catalyst in different reaction conditions, the hydrogenation kinetics, and the recycling of the catalyst as well as the substrate scope were also explored.

Experimental Section

Materials and methods

Unless otherwise stated, all solvents and chemicals used were of commercially available analytical grade and used without further treatment. The surface areas of CN and catalyst Pd/CN were determined by AUTOSORB-1 instrument. BET equation was used to calculate the surface area and pore volume. X-ray power diffraction analysis (XRD) was collected using Ultima TV X-ray diffractometer with Cu Ka radiation (1.54 Å). The X-ray photoelectron spectra (XPS) were obtained by an ESCALAB MARK Ⅱ spherical analyzer using an aluminum-magnesium binode (Al 1486.6 eV, Mg 1253.6 eV) X-ray source. Transmission election microscopy (TEM) characterization was operated on a Hitachi HT-7700 microscope. High-Solution TEM (HRTEM) was performed on Tecnai G2 F30 S-Twin at an acceleration voltage of 300 kV. The particle morphology was visualized using a Gemini scanning electron microscope (SEM). The element analysis was measured on a Vario El elemental analyzer. The Pd content was carried out on a PerkinElmer Optima OES 8000.

Preparation of catalysts

Synthesis of the support material CNx: 9.0 g D-Glucose, 1.2 g additive (poly(ionic liquid)s)[39] and 0.75 g Borax were dissolved in 30 mL water. The mixtures were loaded into a PTFE lined autoclave and treated at 200 °C for 8 h. The resulting black solid was filtered and washed several times with deionized water and ethanol. Then, the solid material was carbonized at 550 °C (heating rate: 3 K min^{-1}, holding time: 4 h) under an inert N_2 atmosphere. After cooling to the room temperature, black carbon material can be got. The process to synthesize carbon sphere without nitrogen (Cs) was almost the same as CNx in absence of poly(ionic liquid)s.

Synthesis of the supported palladium catalysts: We synthesized 1.5%Pd/CN, 1.5%Pd/Cs by ultrasonic-assisted deposition method.[40] 1.5%Pd/MgO, 1.5% Pd/TiO_2 were prepared by wet impregnation according to literature.[41]

Typical procedure for selective hydrogenation and recycling

In a typical reaction, 104.2 mg (0.5 mmol) chalcone, 10 mg Pd/CNx and 5 mL ethanol were precharged in a three-neck flask. The flask was purged with H_2 to remove the air for 3 times, the mixture was then magnetically stirred at 1000 rpm under 1 bar of H_2 at room temperature. After the reaction, contents of the mixture were seperated and analyzed on GC (Shimadzu, GC-2014) equipped with a Rtx-1071 column. Phenethyl phenylketone was used as an internal standard. The catalyst used above was recovered by centrifugation, washed 3 times with ethanol and dried at 80 °C overnight and then used for the next run without any treatment. In order to get the intrinsic kinetic data, chalcone was controlled in low conversion.

Results and Discussion

Catalyst characterization

Elemental analysis indicated that the mesoporous N-doped carbon (denoted as CN$_{,}$) had a N/C atom ratio of about 0.062 (Table S1). SEM and TEM images of CN and Cs demonstrated the hierachically porous network with well-dispersed spherules (Figure 2a, Figure S1, S2). The textural properties of CN and Pd/CN were measured by N_2 adsorption-desorption analysis (Figure 1a). The application of the BET model resulted in the surface area of 424 $m^2 g^{-1}$ for CN. The pore size analysis from nitrogen adsorption by applying density functional theory (DFT) is displayed in Figure S3. The pores in CN have a well-defined micro-mesopore size distribution. The surface area decreased after loading with Pd nanoparticles, but still had considerable value of 193 $m^2 g^{-1}$, suggesting that most of the pores were still accessible. The structures of CN and Pd/CN were investigated by XRD and the patterns were shown in Figure 1b. A broad diffraction peak at around 25° and a weak reflection around 44° were observed for CN and ascribed to the (002) and (100) reflection of the graphitic-type lattice. The diffraction peaks at 40.0°, 46.6° and 68.1° in the XRD patterns could be assigned to the (111), (200) and (220) planes of Pd nanoparticles, respectively.

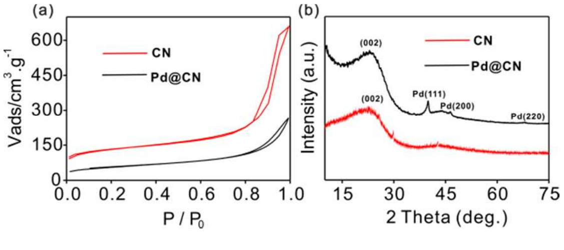

Figure 1. (a) N_2 adsorption/desorption isotherms and (b) XRD patterns of the parent CN and Pd/CN.

The morphologies of Pd/CN composite materials were also unambiguously characterized by TEM. The TEM images evidenced the high and homogeneous dispersion of spheroidal Pd particles with a mean size of 3.2 nm (Figure 2b). The Pd nanoparticles with well-defined lattice fringes in HRTEM image confirmed the (111) crystal plane of Pd, as the crystal plane spacing was measured as 0.220 nm (Figure 2c). To obtain further insight into the structure of the catalyst, XPS investigations were conducted. The Pd 3d XPS spectra in Figure 2d consisted of two asymmetric peaks assigned to Pd $3d_{5/2}$ and Pd $3d_{3/2}$ core levels, which can be fitted using two doublets. The peaks around 335.7 and 340.9 eV were attributed to metallic Pd^0, while those around 337.7 and 343.0 eV correspond to Pd^{2+} species. The percentage of the Pd^0 and Pd^{2+} species was calculated from the relative areas of these peaks. It indicated that Pd^0 was the main metal species on the surface of the as-prepared catalyst (~75%). The amine groups in the carbon carrier are suitable for stabilizing highly dispersed Pd^0 nanoparticles and prevent their oxidation.

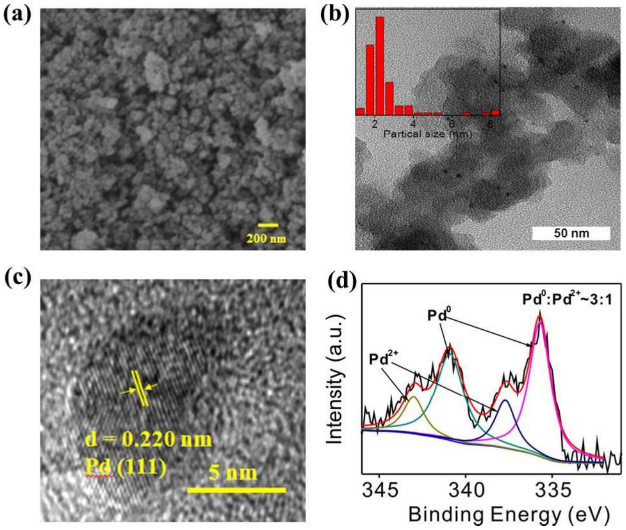

Figure 2. (a) SEM image of the N-doped carbon material, CN. (b) TEM image and particle size distribution, (c) HRTEM image and (d) XPS spectra of Pd/CN.

Catalytic hydrogenation

To illustrate the usefulness of this nanohybrid catalyst Pd/CN, we use chemoselective hydrogenation of chalcone at room temperature under one atmosphere hydrogen pressure as a model reaction.

Effect of solvents

Solvents play a critical role in heterogeneous catalytic hydrogenation and may alter the product distribution.[42, 43] Consequently, the influence of different solvents on the reaction was given priority to investigate.

Table 1 presented the corresponding conversions and selectivities at 35 °C and 1 bar H_2 over Pd/CN, along with the physical and chemical properties of solvents including polarity and solubility of H_2. Although the mechanistic basis of the solvent influences on the heterogeneous hydrogenation is not clear, some conclusions have been rationalized by correlating the reaction rate and selectivity with H_2 solubility or polarity. However, in our reaction system, we could readily achieve conversions of chalcone in the range 88-100%, with >99% selectivities toward dihydrochalcone in various solvents listed below, which was not correlated with either the H_2 solubility or solvent polarity. This phenomenon was also observed in the chemoselective hydrogenation of quinoline.[44] Though chalcone is insoluble in water, we could also get similar activity when compared with other solvents. Doping with N atoms increased the hydrophilic property of the catalyst, which may enhance the catalyst dispersion in water and improve the exposure of the catalyst to the substrate, thereby increasing the catalytic performance. Among the solvents, both toluene and ethanol gave the highest activity. Considering the toxicity of toluene, we selected ethanol as the reaction medium in the subsequent research, which was a cheap and versatile medium.

Table 1. Effect of solvents on the selective hydrogenation of chalcone [a]

Entry	Solvent	Conv. [b] (%)	Sel. [b] (%)	δ[c]	p[d]
1	Toluene	>99	>99	2.75	2.4
2	Dioxane	88	>99	1.95	4.8
3	Ethanol	>99	>99	3.43	4.3
4	DMF	90	>99	-	6.4
5	Acetonitrile	95	>99	-	6.2
6	Water	93	>99	0.81	10.2

[a] Reaction conditions: chalcone (0.5 mmol), Pd (0.28 mol% relative to substrate), solvent (5 mL), temperature (35 °C), H_2 (1 bar pressure), time (2 h). [b] Determined by GC and GC-MS. [c] Solubility of H_2 (10^{-3} mol/L, taken from Hydrogen and Deuterium, Colin L, Young). [d] Solvent polarity.

Effect of reaction temperature

Variation of the reaction temperature had a considerable effect on the reaction conversion, as illustrated in Figure 3a. Complete conversion was achieved with excellent selectivity within 1.7 h at an ambient hydrogen pressure and 35 °C. The reaction was accelerated at higher temperature without any losing of the selectivity, for example, full conversion in 1.2 h was obtained at 45 °C with a high selectivity (>99%). But even at a low temperature of 25 °C, outstanding performance (>99% yield) could be reached after a slightly longer reaction time of 3 h. The smooth completion of chemoselective hydrogenation under mild conditions may provide the possibility for industrial application.

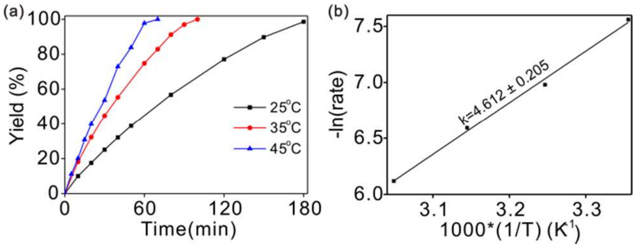

Figure 3. (a) The time-activity profile under different temperatures. Reaction conditions: chalcone (0.5 mmol), Pd (0.28 mol% relative to substrate). (b) Temperature dependence of the rate of reaction in the Arrhenius coordinates for Pd/CN. Reaction conditions: chalcone (1 mmol), Pd (0.28 mol% relative to substrate), CH_3CH_2OH (5 mL), H_2

(1 bar pressure).

Straight lines can be fitted at different temperatures using the data in Figure 3a (conversion below 45%), indicating that the reaction is zero order in chalcone when below 45% conversion (Figure S4). The influence of temperature on the kinetics of the reaction was studied at 25, 35, 45, and 55 °C. To determine the activation energy of the hydrogenation reaction, the data was obtained at low conversions. Based on the linear fit of the Arrhenius plot in Figure 3b, the apparent activation energy (E_a) was found to be 38.3±1.7 kJ/mol, which is consistent with its high catalytic activity, suggesting an easily initiated reaction.

The comparison of various catalysts [a]

To further study the effect of support, the Pd/CN catalyst was compared with several other catalysts including Pd/Cs, Pd/TiO_2, and Pd/MgO under identical conditions (Table 2). The textural properties of different catalysts were listed in Table S2. Among the different catalysts, Pd/CN was found to give the most-active system (Table 2, entry 1). Oxide-supported Pd nanoparticles were not effective for this reaction, affording target product in lower yield (Table 2, entries 3-4). The reasons may arise from the uneven distribution of active position of Pd on the inorganic oxide surface. Particularly worth mentioning was that the performance of Pd/Cs was almost as good as Pd/CN (Table 2, entry 2), which may attribute to the fast diffusion of the reactant or product in hierarchically porous network with well-dispersed small spherules of Cs and CN. Taking into account of the above results, a conclusion may be drawn that the nature of the support has a marked influence in the activity of Pd catalysts for this reaction.

Table 2. Catalytic results for different catalysts [a]

Entry	Catalyst	Conv. [b] (%)	Sel. [b] (%)	TOF (h^{-1})
1	Pd/CN	>99	>99	238.1
2	Pd/Cs	91	>99	216.7
3	Pd/TiO_2	10	>99	23.8
4	Pd/MgO	31	>99	73.8

[a] Reaction conditions: chalcone (0.5 mmol), Pd (0.28 mol% relative to substrate), CH_3CH_2OH (5 mL), temperature (35 °C), H_2 (1 bar pressure),time (1.5 h). [b] Determined by GC.

Reaction kinetics

Mass transfer can play an important role in liquid phase hydrogenations using porous catalysts.[45] Therefore, it is necessary to make sure that mass effects should be ruled out before obtaining reliable kinetic data.[46] To check the true reaction kinetics were not controlled by any of the diffusion processes, a range of different catalyst masses were used to measure the conversion and the stirring speed was varied from 500 to 1000 rpm. No obvious difference in rates of reactions at various stirring speed could be observed.

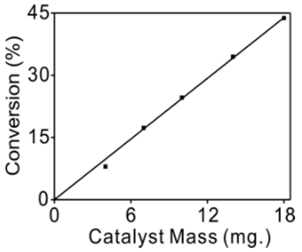

Figure 4. The catalytic activity of 1.5%Pd/CN as a function of catalyst mass, at 35 °C and 1 bar H_2, 0.5 h.

The straight line shown in Figure 4 also elucidated that the external diffusion was not the rate-limiting under the reaction conditions. On the other hand, based on the very small particles of the catalyst used, the role of internal diffusion was estimated to be insignificant. Above all, the smallest catalyst particle size and highest stirring speed (1000 rpm) were adopted to minimize the possibility of mass transfer.

The overall rate of this reaction can be given by the following equation: $r = k[c]^n P_{H_2}^m$, where *k* is the overall rate constant, *n* is the order with respect to chalcone and *m* is the order corresponding to hydrogen. The reaction order *n* and *m* were determined by double logarithmic plots of the initial TOF and chalcone concentration or H_2 pressure. As can be seen in Figure 5a, the TOF remained static as the initial chalcone concentration was increased from 0.1 to 1.0 M, indicating a typical characteristic of zero-order respect to chalcone. The conclusion is also coincided with Figure 3a, namely, the reaction is zero order in chalcone when below 45% conversion. The zero-order respect to chalcone implies a surface largely covered with reactive hydrocarbon intermediates.[47] Over a hydrogen pressure range 2-15 bar, the initial TOF showed a lower exponential dependence on P_{H_2} of 0.38 (see Figure 5b). As a result, a power law rate expression was derived: $r = k[c]^0 P_{H_2}^{0.38}$.

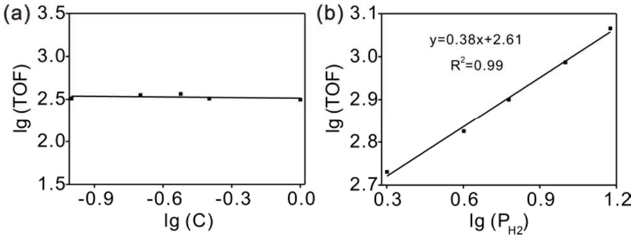

Figure 5. Dependence of initial TOF on chalcone concentration (a) and H_2 pressure (b) for chalcone hydrogenation on Pd/CN.

The reusability of the catalyst

For recycling study, chemoselective hydrogenation of chalcone was conducted maintaining the same reaction conditions except using the recovered catalyst. We tested the catalytic activity of Pd/CN and Pd/Cs in successive runs and compiled in Figure 6. To our delight, Pd/CN was recycled up to 8 times with little loss of activity, which was prerequisite for practical applications. Nevertheless, the Pd/Cs displayed a noticeable inactivation during the recycling, indeed only giving a 24% conversion at the third recycle.

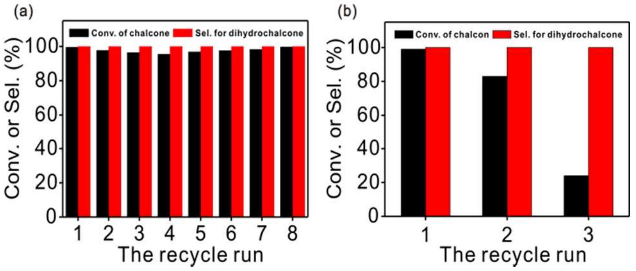

Figure 6. (a) Reuse of Pd/CN and (b) Reuse of Pd/Cs. (35 °C, 2.5 h).

The TEM images of Pd/CN after 8 time recycles revealed the particle size of ~3.5 nm, almost the same as the fresh catalyst (Figure S5), which indicated aggregation-free after reused. The slightly decreased activity of Pd/CN was primarily due to minor metal leaching as manifested in Table S3 during the separation and purification operation. A hot filtration experiment indicated that the leached species in the filtrate made no difference in the conversion of chalcone (Figure S6). Though the mean particle size of reused Pd/Cs remained about the same as the fresh one (Figure S5), the palladium content declineded dramatically to 0.82 wt% from 1.29 wt% in the third recycle, leading to the conspicuous loss in activity.

Notably, the palladium content of Pd/Cs dropped faster than Pd/CN, which was ascribed to the versatile nitrogen in the catalyst support. XPS spectra suggested that the nature and the content of nitrogen species in the surface of the fresh and recycled catalyst are almost the same (Figure S7). Nitrogen is strongly electronegative and usually has a lone pair of electrons, the nitrogen functionalities on the surface might act as Lewis base sites and are expected to be more effective in retaining metal nanoparticles. Simultaneously, N-doped carbon material enriches the electron density of the metallic Pd and accelerates the reaction, as compared to Pd/Cs.

The possible reaction mechanism

More studies have focused on the reaction pathway and mechanism about acrolein and crotonaldehyde. Though there are no similar studies for chalcone, some generalizations can be made based on the experimental data and the theoretical results those have been reported. The extended Huckel calculations suggest that the narrower the width of the metal d-band, the greater the interaction of the metal surface with the conjugated olefinic bond compared to the carbonyl bond (the width of the metal d-band: Pd < Pt < Os).[21] DFT calculations[48] and the HREELS study[49] have shown that maleic anhydride interacts with the Pd (111) surface via the C=C bond. On the other hand, the C=C bond may be adsorbed almost parallel to the metal surface because the mean particle size of Pd are as small as 3.2 nm. Presumably, the close interaction between Pd and C=C bond benefited the high catalytic performance in our system. More importantly, the hierarchically structured porous materials may modify the adsorption properties of the metal surface itself and can provide large surface areas for reaction, interfacial transport, or dispersion of active sites at different length scales of pores and shorten diffusion paths or reduce the diffusion effect[33]. Scheme 2 illustrates the proposed step sequence of the chemoselective hydrogenation process. In the initial step, the substrate interacts with the Pd surface via the C=C bond and H_2 is dissociated by the electronically supported Pd. Subsequently, the C=C bond is selectively hydrogenated by the attack of the activated hydrogen atom. Because of the high diffusion pathways and shortened diffusion path in the hierarchical mesoporous channels, the formed saturated carbonyls leave the surface of the catalyst quickly, being replaced by a new molecule and avoiding further hydrogenation to saturated alcohol.

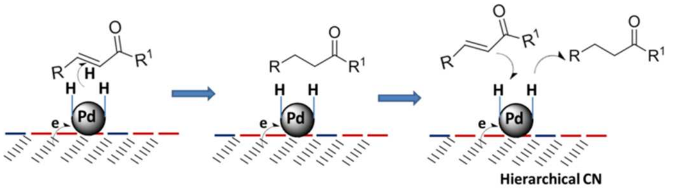

Scheme 2. Possible reaction mechanism of selective hydrogenation process over Pd/CN

Catalytic performance for various α, β-unsaturated carbonyls

The general scope of Pd/CN was tested in the reduction of a series of α, β-unsaturated carbonyls with the results summarized in Table 3. Gratifyingly, full conversion was achieved in all cases, and the selectivities toward corresponding product were excellent (>99%). Apart from simple α, β-unsaturated aldehydes such as butenal and citral (Table 3, entries 1-2), also α, β-unsaturated ketones, like benzalacetone and chalcone were selectively reduced (Table 3, entries 3-4). Furthermore, remarkable chemoselectivity was demonstrated in the hydrogenation of C=C bond in presence of other reducible groups such as ester group, carboxyl, amino and nitrile group at room temperature with 1 bar hydrogen pressure (Table 3, entries 5-9). In view of the results, it appeared that steric effects imposed by substituent groups on the C atoms in the C=C bond did not have an influence on the intramolecular selectivity, which was exactly in line with the conclusion reported by Utpal K. Singh *et al*.[50]

Table 3. Selective hydrogenation of various α, β-unsaturated carbonyls [a]

Entry	Substrate	Product	Time (h)	Yield. (%)	TOF (h^{-1})
1			0.5	>99	714.2
2			4	>99	89.2
3			2	>99	178.6
4			2.5	>99	160
5			0.5	>99	714.2
6			0.5	>99	714.2
7			0.5	>99	714.2
8			0.5	>99	714.2
9			2	>99	178.6

[a] Reaction conditions: substrate (0.5 mmol), Pd (0.28 mol% relative to substrate), CH_3CH_2OH (5 mL), 30 °C, H_2 (1 bar pressure). [b] Determined by GC and GC-MS.

Conclusions

In summary, the Pd/CN shows distinctly high catalytic activity in the chemoselective hydrogenation of C=C band in various α, β-unsaturated carbonyls at mild conditions (303 K, atmospheric H_2). It can be reused for 8 times without significant loss of catalytic activity and selectivity, much better than Pd/Cs. The considerable catalytic performance is stemed from the hierarchically porous network and incorporation of nitrogen atoms. The hierarchically porous network and mesoporous character enormously inhibit the mass transfer limitation of the reactant to the active sites, promote the free diffusion of molecules and shorten diffusion distances in the channels. The introduction of nitrogen atoms leads not only to a very stable and uniform dispersion of Pd but also to additional electronic activation of the metal nanoparticles. This synthesis strategy (by modulation of pore structure and introduction of heteroatoms in catalyst support) can open routes for the design of many more powerful catalysts.

Acknowledgements

Financial support from the National Natural Science Foundation of China (21376208 & U1162124), the Zhejiang Provincial Natural Science Foundation for Distinguished Young Scholars of China (LR13B030001), the Specialized Research Fund for the Doctoral Program of Higher Education (J20130060), the Fundamental Research Funds for the Central Universities, the Program for Zhejiang Leading Team of S&T Innovation, and the Partner Group Program of the Zhejiang University and the Max-Planck Society are greatly appreciated.

Notes and references

Carbon Nano Materials Group, ZJU-NHU United R&D Center, Department of Chemistry, Zhejiang University, Hangzhou 310028, P. R. China
Fax: +86 571-87951895; E-mail: chemwy@zju.edu.cn

1. G. Neri, L. Mercadante, A. Donato, A. M. Visco and S. Galvagno, *Catal. Lett.*, 1994, 29, 379-386.
2. M. Englisch, A. Jentys and J. A. Lercher, *J. Catal.*, 1997, 166, 25-35.
3. M. D. Bhor, A. G. Panda, S. R. Jagtap and B. M. Bhanage, *Catal. Lett.*, 2008, 124, 157-164.
4. N. Mahata, A. F. Cunha, J. J. M. Orfao and J. L. Figueiredo, *Chem. Eng. J.*, 2012, 188, 155-159.
5. Y. Wang, J. Yao, H. R. Li, D. S. Su and M. Antonietti, *J. Am. Chem. Soc.*, 2011, 133, 2362-2365.
6. Y. H. Niu, L. K. Yeung and R. M. Crooks, *J. Am. Chem. Soc.*, 2001, 123, 6840-6846.
7. F. A. Khan, A. Vallat and G. Suss-Fink, *J. Mol. Catal. A: Chem.*, 2012, 355, 168-173.
8. M. L. Kantam, T. Parsharamulu and S. V. Manorama, *J. Mol. Catal. A: Chem.*, 2012, 365, 115-119.
9. B. P. S. Chauhan, J. S. Rathore and T. Bandoo, *J. Am. Chem. Soc.*, 2004, 126, 8493-8500.
10. D. B. Bagal, Z. S. Qureshi, K. P. Dhake, S. R. Khan and B. M. Bhanage, *Green Chem.*, 2011, 13, 1490-1494.
11. T. Gallert, M. Hahn, M. Sellin, C. Schmöger, A. Stolle, B. Ondruschka, T. F. Keller and K. D. Jandt, *ChemSusChem*, 2011, 4, 1654-1661.
12. S. Morrissey, I. Beadham and N. Gathergood, *Green Chem.*, 2009, 11, 466-474.
13. H. Hagiwara, T. Nakamura, T. Hoshi and T. Suzuki, *Green Chem.*, 2011, 13, 1133-1137.
14. Z. Baan, Z. Finta, G. Keglevich and I. Hermecz, *Green Chem.*, 2009, 11, 1937-1940.
15. A. Mori, Y. Miyakawa, E. Ohashi, T. Haga, T. Maegawa and H. Sajiki, *Org. Lett.*, 2006, 8, 3279-3281.
16. Y. C. Hong, K. Q. Sun, G. R. Zhang, R. Y. Zhong and Q. Xu, *Chem. Commun.*, 2011, 47, 1300-1302.
17. W. W. Lin, H. Y. Cheng, L. M. He, Y. C. Yu and F. Y. Zhao, *J. Catal.*, 2013, 303, 110-116.
18. Y. E. Wu, S. F. Cai, D. S. Wang, W. He and Y. D. Li, *J. Am. Chem. Soc.*, 2012, 134, 8975-8981.
19. B. H. Zhao, J. G. Chen, X. Liu, Z. W. Liu, Z. P. Hao, J. L. Xiao and Z. T. Liu, *Ind. Eng. Chem. Res.*, 2012, 51, 11112-11121.
20. N. Morimoto, S. Yamamoto, Y. Takeuchi and Y. Nishina, *Rsc Adv.,* 2013, 3, 15608-15612.
21. F. Delbecq and P. Sautet, *J. Catal.*, 1995, 152, 217-236.
22. V. Pallassana and M. Neurock, *Chem. Eng. Sci.*, 1999, 54, 3423-3431.
23. H. G. Manyar, B. Yang, H. Daly, H. Moor, S. McMonagle, Y. Tao, G. D. Yadav, A. Goguet, P. Hu and C. Hardacre, *Chemcatchem*, 2013, 5, 506-512.
24. K. Q. Sun, Y. C. Hong, G. R. Zhang and B. Q. Xu, *Acs Catal.* 2011, 1, 1336-1346.
25. S. Handjani, E. Marceau, J. Blanchard, J.-M. Krafft, M. Che, P. Maeki-Arvela, N. Kumar, J. Waerna and D. Y. Murzin, *J. Catal.*, 2011, 282, 228-236.
26. R. J. White, R. Luque, V. L. Budarin, J. H. Clark and D. J. Macquarrie, *Chem. Soc. Rev.*, 2009, 38, 481-494.
27. J. P. Tessonnier, L. Pesant, G. Ehret, M. J. Ledoux and C. Pham-Huu, *Appl. Catal., A*, 2005, 288, 203-210.
28. P. Makowski, R. Demir Cakan, M. Antonietti, F. Goettmann and M.-M. Titirici, *Chem. Commun.*, 2008, DOI: 10.1039/B717928F, 999-1001.
29. P. Serp, M. Corrias and P. Kalck, *Appl. Catal., A*, 2003, 253, 337-358.
30. H. Bernas, I. Simakova, I. P. Prosvirin, P. Maki-Arvela, R. Leino and D. Y. Murzin, *Catal. Lett.*, 2012, 142, 690-697.
31. C. Pham-Huu, N. Keller, L. J. Charbonniere, R. Ziessle and M. J. Ledoux, *Chem. Commun.*, 2000, DOI: 10.1039/b005306f, 1871-1872.
32. C. D. Liang, Z. J. Li and S. Dai, *Angew. Chem., Int. Ed.*, 2008, 47, 3696-3717.
33. Y. Li, Z. Y. Fu and B. L. Su, *Adv. Funct. Mater.*, 2012, 22, 4634-4667.
34. Y. Zhu, Z. L. Hua, Y. D. Song, W. Wu, X. X. Zhou, J. Zhou and J. L. Shi, *J. Catal.*, 2013, 299, 20-29.
35. X. Xu, Y. Li, Y. Gong, P. Zhang, H. Li and Y. Wang, *J. Am. Chem. Soc.*, 2012, 134, 16987-16990.
36. C. Han, J. Wang, Y. Gong, X. Xu, H. Li and Y. Wang, *J. Mater. Chem. A,* 2014, 2, 605-609.
37. P. F. Zhang, Y. T. Gong, H. R. Li, Z. R. Chen and Y. Wang, *Nat. Commun.,* 2013, 4.
38. P. Zhang, J. Yuan, T.-P. Fellinger, M. Antonietti, H. Li and Y. Wang, *Angew. Chem., Int. Ed.,* 2013, 52, 6028-6032.
39. T. P. Fellinger, R. J. White, M. M. Titirici and M. Antonietti, *Adv. Funct. Mater.*, 2012, 22, 3254-3260.
40. Y. Li, X. Xu, P. Zhang, Y. Gong, H. Li and Y. Wang, *RSC Adv.,* 2013, 3, 10973-10982.
41. U. R. Pillai and E. Sahle-Demessie, *Green Chem.*, 2004, 6, 161-165.
42. R. J. Hou, T. F. Wang and X. C. Lan, *Ind. Eng. Chem. Res.*, 2013, 52, 13305-13312.
43. S. Mukherjee and M. A. Vannice, *J. Catal.*, 2006, 243, 108-130.
44. Y. T. Gong, P. F. Zhang, X. Xu, Y. Li, H. R. Li and Y. Wang, *J. Catal.*, 2013, 297, 272-280.
45. G. Zhang, B. L. Scott and S. K. Hanson, *Angew. Chem., Int. Ed.,* 2012, 51, 12102-12106.

46. S. Mahmoud, A. Hammoudeh, S. Gharaibeh and J. Melsheimer, *J. Mol. Catal. A: Chem.*, 2002, 178, 161-167.
47. J. P. Breen, R. Burch, J. Gomez-Lopez, K. Griffin and M. Hayes, *Appl. Catal., A*, 2004, 268, 267-274.
48. V. Pallassana, M. Neurock and G. W. Coulston, *J. Phys. Chem. B*, 1999, 103, 8973-8983.
49. C. Xu and D. W. Goodman, *Langmuir*, 1996, 12, 1807-1816.
50. U. K. Singh and M. A. Vannice, *J. Catal.*, 2001, 199, 73-84.